Journal of Biomolecular NMR, **16:** 279–289, 2000.
KLUWER/ESCOM

Characterization of the hydrogen bond network in guanosine quartets by internucleotide $^{3h}J_{NC'}$ and $^{2h}J_{NN}$ scalar couplings

Andrew J. Dingley[a,b], James E. Masse[c], Juli Feigon[c,*] & Stephan Grzesiek[d,*]
[a]*Institute of Physical Biology, Heinrich-Heine-Universität, D-40225 Düsseldorf, Germany;* [b]*Institute of Structural Biology, IBI-2, Forschungszentrum Jülich, D-52425 Jülich, Germany;* [c]*Department of Chemistry and Biochemistry and Molecular Biology Institute, University of California, Los Angeles, CA 90095-1569, U.S.A.;* [d]*Department of Structural Biology, Biozentrum, University of Basel, CH-4056 Basel, Switzerland*

Received 1 December 1999; Accepted 19 January 2000

Key words: base pairs, DNA, hydrogen bond, nucleic acid, quadruplex, scalar coupling

Abstract

Scalar coupling correlations across hydrogen bonds with carbonyl groups as acceptors have been observed in a variety of proteins, but not in nucleic acids. Here we present a pulse scheme that allows such an observation and quantification of trans-hydrogen bond $^{3h}J_{NC'}$ correlations in nucleic acid base pairs, between the imino nitrogen ^{15}N1 and the carbonyl ^{13}C6 nuclei within the guanine quartets of the Oxy-1.5 DNA-quadruplex. Intra- and internucleotide N-H$\cdots$O=C connectivities can be traced around each guanine quartet, allowing the hydrogen bonding partners to be unambiguously assigned. Absolute values of the $^{3h}J_{NC'}$ couplings are approximately 0.2 Hz as quantified by a selective long-range H(N)CO experiment and are thus on average smaller than the analogous $^{3h}J_{NC'}$ couplings observed in proteins. In addition, an improved version of the pseudo-heteronuclear H(N)N-COSY [Majumdar et al. (1999) *J. Biomol. NMR*, **14**, 67–70] is presented which allows simultaneous detection of the ^{15}N-donor and ^{15}N-acceptor resonances connected by $^{2h}J_{NN}$ couplings in hydrogen bonds involving amino groups. Using this experiment, values ranging between 6 and 8 Hz are determined for the $^{2h}J_{NN}$ couplings between ^{15}N2 and ^{15}N7 nuclei in the guanine quartet. These values are not strongly influenced by the presence of a significant amount of chemical exchange broadening due to amino group rotations.

Introduction

Tertiary structures of nucleic acids commonly contain not only hydrogen bonds within canonical Watson–Crick base pairs but also in a wide variety of non-standard base pairs as well as between bases and sugars, sugars and sugars, and from bases or sugars to phosphates (Saenger, 1984; Gesteland and Atkins, 1993; Cate et al., 1996). In solution structures of folded nucleic acids such hydrogen bonding networks have been deduced conventionally from the observation of NOEs, slowly exchanging imino protons, proton and nitrogen chemical shifts, and in some cases from appropriate distances and angles in the initial structures (Varani et al., 1996; Dieckmann and Feigon, 1997; Butcher et al., 1999). Since the few long-range interactions in helical and folded nucleic acids generally involve hydrogen bonds, in almost all nucleic acid structure calculations it has been necessary to use explicit hydrogen bond restraints at some stage in the structure refinement. Erroneous assumptions of such restraints can easily lead to errors in the final structures, as discussed by Allain and Varani (1995).

These problems can be avoided by direct detection of hydrogen bonds via measurement of electron-mediated scalar couplings between donor and acceptor atoms (Blake et al., 1992a, b; Crabtree et al., 1996; Dingley and Grzesiek, 1998; Kwon and Danishefsky, 1998; Pervushin et al., 1998; Shenderovich et al., 1998; Cordier et al., 1999; Cordier and Grzesiek, 1999; Cornilescu et al., 1999a, b; Dingley et al.,

*To whom correspondence should be addressed. E-mail: Stephan.Grzesiek@unibas.ch (S.G.); feigon@mbi.ucla.edu (J.F.)

1999; Golubev et al., 1999; Wöhnert et al., 1999). The demonstration of a substantial scalar coupling between donor and acceptor nitrogens for the hydrogen-bonded imino groups in Watson–Crick base pairs thus provides a practical new tool to obtain structural information for nucleic acids (Dingley and Grzesiek, 1998; Pervushin et al., 1998). The very existence of the couplings indicates an overlap of donor, hydrogen, and acceptor electronic wave functions and suggests a limited covalent character of the hydrogen bond (Pauling, 1949; Isaacs et al., 1999; Smirnov et al., 1999). Furthermore, quantum chemical calculations quantitatively reproduce the experimental trans-hydrogen bond $^{2h}J_{NN}$ and $^{1h}J_{HN}$ scalar couplings, covalent $^{1}J_{HN}$ couplings, and imino proton chemical shifts for both Watson–Crick and Hoogsteen base pairs in ^{13}C,^{15}N-labeled DNA and RNA as a function of hydrogen bond lengths (Dingley et al., 1999; Scheurer and Brüschweiler, 1999). This suggests that the size of the scalar couplings will also be a useful parameter for distance restraints in nucleic acid structure calculations.

We wished to extend these measurements to other non-Watson–Crick base pairs in nucleic acid structures that involve hydrogen bonds with carbonyl oxygens as acceptors or amino nitrogens as donors. For these studies, we used the oligonucleotide d($G_4T_4G_4$) (Oxy-1.5) which dimerizes to form a C2-symmetric quadruplex (Smith and Feigon, 1992; Schultze et al., 1994). This Oxy-1.5 quadruplex contains the repeat sequence d(T_4G_4) found in *Oxytricha nova* telomeres. Quadruplexes which form from such telomere repeats have been shown to inhibit the riboprotein telomerase which replicates the chromosome ends (Zahler et al., 1991). Although the biological role of such quadruplexes remains to be established, proteins which bind to quadruplexes and/or facilitate their formation have been identified (Fang and Cech, 1993a, b; Giraldo and Rhodes, 1994). The solution structure of the Oxy-1.5 quadruplex has been solved and shows that the 16 guanine bases of the two monomers build a stack of four hydrogen-bonded guanine quartets (Figure 1A) (Smith and Feigon, 1992; Schultze et al., 1994). The four thymines of each monomer form ordered loops connecting diagonally opposed corners of the bottom and top G-quartets such that each consecutive G_4-strand has one parallel and one anti-parallel G_4-strand as its neighbor. A crystal structure of the Oxy-1.5 quadruplex also contains four stacked G-quartets, but the topology of the dimer differs in that the loops span the edge of a quartet at each end of the helix (Kang et al.,

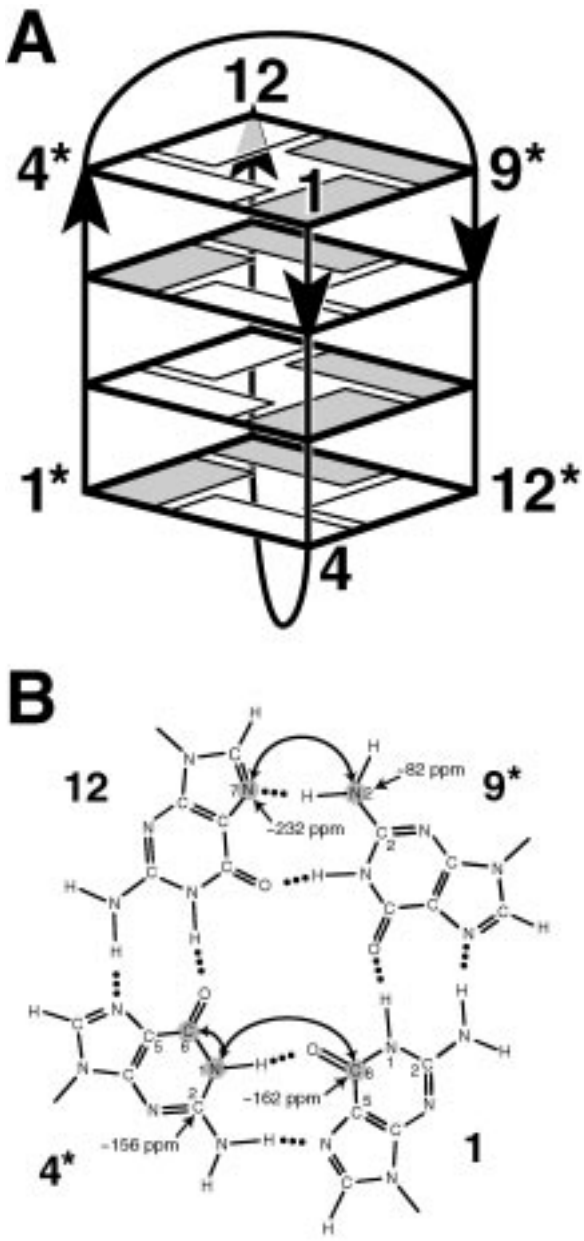

Figure 1. (A) Schematic structure of the Oxy-1.5 quadruplex formed by two d($G_4T_4G_4$) strands. The strand direction along each edge of the quadruplex is indicated by arrows. Guanines are shown as white (*syn* nucleotide) and shaded (*anti* nucleotide) rectangles. The thymines are in the loops that span the end quartets (Smith and Feigon, 1992; Schultze et al., 1994). Residue numbers for the second strand are indicated by asterisks. (B) Chemical structure of the top planar G-quartet. Relevant chemical shift information and J-coupling connectivities are indicated for the observation of $^{3h}J_{N1C6}$ and $^{2h}J_{N2N7}$ trans-hydrogen bond scalar couplings. Shading indicates ^{13}C and ^{15}N nuclei which are observed in the selective long-range H(N)CO ($^{3h}J_{N1C6}$) or the phase coherent heteronuclear H(N)N-COSY ($^{2h}J_{N2N7}$) experiments.

1992). However, a more recent crystal structure of the Oxy-1.5 quadruplex is essentially identical to the solution structure (M. Horvath and S. Schultze, personal communication).

The hydrogen-bonding scheme for G-quartets (Figure 1B) was first proposed over 25 years ago (reviewed in Guschlbauer et al. (1990)). Experimental verification of the Oxy-1.5 quadruplex structure in solution proved extremely difficult based solely on the information obtained from internucleotide NOEs and required the use of oligonucleotides containing modified bases to verify the hydrogen-bonding partners (Smith and Feigon, 1993). Here we present a pulse scheme that allows the first experimental observation and quantification of trans-hydrogen bond $^{3h}J_{NC'}$ correlations in nucleic acid base pairs, between the imino nitrogen ^{15}N1 and the carbonyl ^{13}C6 nuclei within the guanine quartets. We also report the quantification of the $^{2h}J_{N2N7}$ couplings in the G-quartet by an improved version of the pseudo-heteronuclear H(N)N-COSY (Majumdar et al., 1999) which allows a simultaneous detection of the N2 and N7 resonances such that the value of the coupling can be derived directly from the ratio of the N2 and N7 peak intensities. The results show that the G-quartet hydrogen-bond network can be verified with relative ease by the detection of trans-hydrogen bond scalar couplings involving carbonyl and amino groups, and provide new data on the strengths of these couplings in nucleic acids.

Experimental

The uniformly ^{13}C,^{15}N-labeled d($G_4T_4G_4$) quadruplex was synthesized as described (Masse et al., 1998). NMR experiments were carried out on a Shigemi microcell sample of 250 μl volume containing 1.5 mM DNA quadruplex (3 mM oligomer), 50 mM NaCl, and 95% H_2O/5% D_2O at pH 7.2. NMR data were acquired at either 298 K ($^{3h}J_{NC'}$ experiment) or 274 and 288 K ($^{2h}J_{NN}$ experiment) on a Bruker DMX-600 NMR spectrometer, equipped with a standard 5 mm triple-axis pulsed field gradient ^{1}H/^{15}N/^{13}C probehead optimized for ^{1}H detection.

The long-range, water flip-back, selective pulse, quantitative-$J_{NC'}$ H(N)CO experiment depicted in Figure 2 was used to measure heteronuclear ^{15}N–^{13}C scalar coupling constants for the DNA quadruplex. The data matrices consisted of 25* (t_1) × 1024* (t_2) data points (where n* refers to complex points) with acquisition times of 40 ms (t_1) and 77 ms (t_2). A total of 2176 scans per complex t_1 increment were collected for pulse scheme A, whereas 32 scans were accumulated in the reference experiment B (Figure 2). The total measuring time for such a pair of experiments was 64.5 h.

The modified quantitative-J_{NN} H(N)N-COSY experiment depicted in Figure 4 was used to measure the homonuclear ^{15}N–^{15}N trans-hydrogen bond coupling constants between the far upfield (∼82 ppm) donor ^{15}N2 amino nitrogen and the far downfield (∼232 ppm) acceptor ^{15}N7 aromatic nitrogen nuclei of the G–G base pairs of the DNA quadruplex. The data matrix consisted of 50* (t_1) × 1024* (t_2) data points with acquisition times of 44 ms (t_1) and 77 ms (t_2). A total of 256 scans per complex t_1 increment were collected.

NMR data sets were processed using the program NMRPipe (Delaglio et al., 1995) and peak positions and integrals were determined with the program PIPP (Garrett et al., 1991) and the time domain fitting routine nlinLS contained in the NMRPipe package. For determining the hydrogen-bond distances and angles, hydrogens were added to the Oxy-1.5 crystal structure with the program XPLOR (Brünger, 1992), using ideal covalent geometry and a guanosine N1-H1 distance of 1.04 Å.

Results

$^{3h}J_{NC'}$ couplings

Each G-quartet of Oxy-1.5 (Figure 1B) contains four hydrogen bonds between the guanosine imino groups (H1-N1) and the carbonyl groups (O6=C6). Trans-hydrogen bond couplings to the ^{13}C-nucleus of carbonyl groups have been reported previously for proteins, but not for nucleic acids. Depending on the hydrogen bond length (Cordier et al., 1999; Cordier and Grzesiek, 1999; Cornilescu et al., 1999a, b; Wang et al., 1999), absolute values for such $^{2h}J_{HC'}$ and $^{3h}J_{NC'}$ couplings range between 0.1 and 0.9 Hz. The couplings to the carbonyl ^{13}C nuclei are therefore considerably smaller than in the case where the acceptor nucleus itself is observed, e.g. the $^{2h}J_{NN}$ (6–10 Hz) and $^{1h}J_{HN}$ (2–4 Hz) couplings in many nucleic acid base pairs.

In the present study, we show that trans-hydrogen bond $^{3h}J_{NC'}$ couplings between the donor imino ^{15}N1 and the acceptor carbonyl ^{13}C6 are also detectable in the guanine quartets of Oxy-1.5. This is achieved by a selective long-range H(N)CO-experiment (Fig-

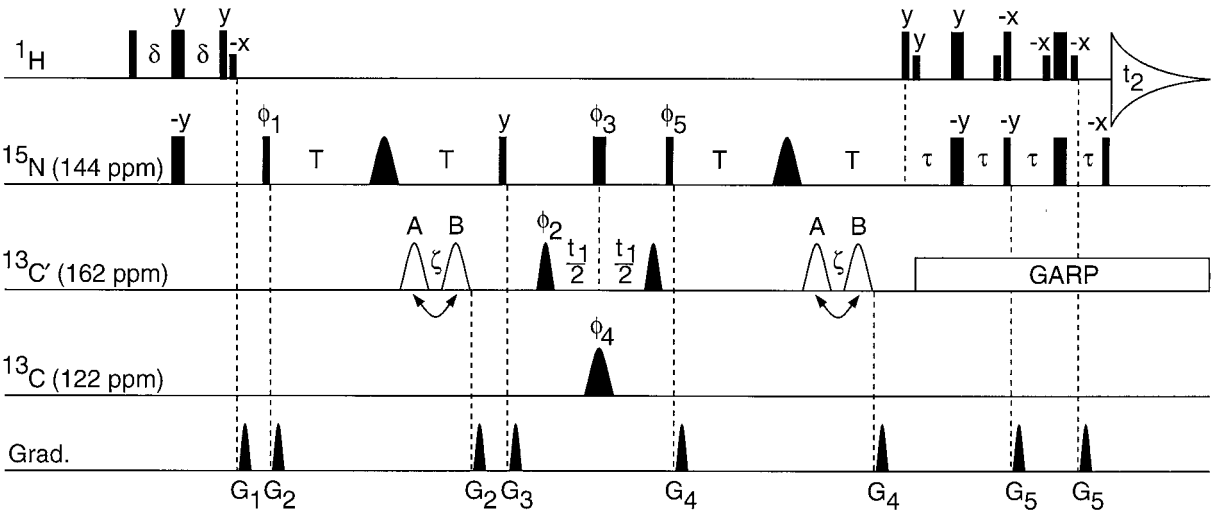

Figure 2. Pulse sequence of the long-range quantitative-J_{NC} H(N)CO experiment. Narrow and wide pulses correspond to flip angles of 90° and 180°, respectively, and all pulse phases are x unless specified. Carrier positions are ^1H_2O (^{1}H), 144.1 ppm (^{15}N), and 162.3 ppm (^{13}C). All regular ^{1}H pulses are applied at an RF field strength of 29 kHz, whereas rectangular low-power ^{1}H pulses are applied using $\gamma_H B_1/2\pi = 200$ Hz. All regular ^{15}N pulses are applied at an RF field strength of 5.9 kHz. The shaped ^{15}N 180° pulses at the midpoint of each 2T period have a G3 (Emsley and Bodenhausen, 1990) amplitude profile, with durations of 7.2 ms, corresponding to a refocusing bandwidth of ± 3 ppm. The shaped ^{13}C 180° pulses (open) at the midpoint of each 2T period have a G3 amplitude profile, with durations of 8.7 ms, corresponding to an inversion bandwidth of ± 1 ppm. The ^{13}C 90° pulses bracketing the t_1 period and the ^{13}C 180° decoupling pulse centered in the t_1 period have the shape of the center lobe of a (sin*x*)/*x* function and durations of 150 and 300 μs, respectively. GARP decoupling ($\gamma_C B_3/2\pi = 3.3$ kHz) on the ^{13}C channel was applied during the two reverse INEPT and acquisition periods. Delay durations: T = 80 ms ≈ $1/^1J_{N1C6}$; δ = 2.25 ms; τ = 2.7 ms; ζ = 20 ms. Phase cycling: ϕ_1 = 8(x), 8(−x); ϕ_2 = 4(x), 4(−x); ϕ_3 = 32(x), 32(−x); ϕ_4 = 16(x), 16(−x); ϕ_5 = (y, x, −y, −x) =: R; receiver = R, −R, −R, R. Quadrature detection in the t_1 dimension was achieved by incrementing ϕ_2 in the States-TPPI manner. Gradients are sine-bell shaped, with an absolute amplitude of 25 G/cm at their center and durations of $G_{1,2,3,4,5}$ = 2.5, 3.75, 2.7, 0.88, and 0.4 ms. For the quantification of $J_{NC'}$ couplings, two independent experiments are performed with the ^{13}C 180° shaped pulses (open) applied at either position A or B. Cross peaks observed for experiment A are mainly the result of small ^{15}N to ^{13}C couplings (such as $^{3h}J_{NC'}$) which evolve during the full period 2T. Cross peaks observed in scheme B (reference) are a result of the intranucleotide $^1J_{NC'}$ couplings which are active during the period 2(T − ζ).

ure 2). The experiment is similar to the recently published long-range $J_{NC'}$ H(N)CO experiment with TROSY detection (Pervushin et al., 1997) which was used to measure the analogous $^{3h}J_{NC'}$ couplings in a large perdeuterated protein (Wang et al., 1999). In contrast to proteins, in nucleic acids which are uniformly ^{13}C and ^{15}N enriched, the detection of small, trans-hydrogen bond $^{3h}J_{NC'}$ correlations is considerably more difficult due to the presence of relatively large one-, two-, and three-bond intranucleotide ^{15}N–^{13}C couplings (Ippel et al., 1996). To avoid loss of magnetization due to these ^{15}N–^{13}C intranucleotide scalar couplings, band-selective pulses are used such that magnetization transfer occurs uniquely between the imino ^{15}N1 and the carbonyl ^{13}C6 spins. In particular, highly selective ^{13}C inversion pulses are necessary to avoid the unwanted intranucleotide one-bond (∼20 Hz) magnetization transfer from the ^{15}N1 to the ^{13}C2 nucleus which is very close in frequency (∼156 ppm) to the carbonyl ^{13}C6 nucleus (∼162 ppm, Figure 1B). For this reason, the inversion profile of the 180° ^{13}C G3 pulse was adjusted such that it covers only a bandwidth of approximately ± 1 ppm around the ^{13}C6 resonances and leaves ^{13}C spins more than 3 ppm from the ^{13}C carrier essentially unaffected. Similarly, the selective 180° ^{15}N G3 pulse (± 3 ppm) during each of the 2T periods ensures that the intranucleotide homonuclear two-bond J_{NN} coupling of ∼ 2 Hz (Dingley et al., 1999) between the imino ^{15}N1 and ^{15}N3 nuclei is also refocused.

In contrast to a standard HNCO experiment in proteins, the pulse scheme in Figure 2 uses long nitrogen to carbonyl de/rephasing periods of a length 2T ≈ $2/^1J_{N1C6}$ (160 ms). This has the effect of approximately refocusing the covalent $^1J_{N1C6}$ coupling (∼12.5 Hz), while leaving the magnetization transfer across the hydrogen bond by the much smaller $^{3h}J_{NC'}$ coupling active. In principle, such refocusing is achieved by any choice of 2T ≈ $n/^1J_{N1C6}$, with *n* being an integer. However, the maximal sensitivity for the

cross peaks is obtained when 2T is set to values close to the transverse relaxation time of the ^{15}N1 nucleus. It is interesting to note that for the extended dephasing periods used in the experiment, the ^{15}N1 transverse relaxation contains a significant contribution due to scalar relaxation of the second kind (Abragam, 1961) resulting from the finite lifetimes of the longitudinal ^{13}C6 and ^{13}C2 magnetization. Considering only the active couplings to the ^{13}C6-nucleus, the intensity of a cross peak between the imino proton and the acceptor carbonyl carbon in the long-range selective pulse H(N)CO (Figure 2, scheme A) will be proportional to $\sin^2(2\pi^{3h}J_{NC'}T)*\cos^2(2\pi^{1}J_{N1C6}T)$. As explained previously (Cordier and Grzesiek, 1999), the value of $^{3h}J_{NC'}$ can be quantified by comparing the cross-peak intensities to the intensities of a reference spectrum (Figure 2, scheme B) which is recorded with the selective ^{13}C′ 180° pulses shifted by a delay $\zeta = 20$ ms $\approx 1/(4*^{1}J_{N1C6})$ relative to the position of the ^{15}N 180° pulses in the middle of the INEPT transfer intervals (Figure 2, scheme B). In this reference experiment, predominantly intranucleotide $^{1}J_{N1C6}$ correlations are measured and the value of $^{3h}J_{NC'}$ is determined from the relation:

$$\sqrt{\frac{I_{hbond}}{I_{ref}}} = \frac{\sin(2\pi^{3h}J_{NC'}T) * \cos(2\pi^{1}J_{N1C6}T)}{\sin(2\pi^{1}J_{N1C6}[T-\zeta]) * \cos(2\pi^{3h}J_{NC'}[T-\zeta])} \approx 2\pi^{3h}J_{NC'}T \quad (1)$$

where the approximation holds for small values of $^{3h}J_{NC'}$ such that $|2\pi^{3h}J_{NC'}T| \ll 1$ and values of $^{1}J_{N1C6}$ close to 12.5 Hz.

Figure 3A shows the result of such a 65 h long-range selective pulse $J_{NC'}$ H(N)CO experiment (Figure 2, pulse scheme A) for the DNA quadruplex. Eight trans-hydrogen bond $^{3h}J_{NC'}$ correlations are visible between different donor imino ^{15}N1 and acceptor carbonyl ^{13}C6 nuclei. These eight correlations correspond to the total number of 16 guanosine N1-H1$\cdots$O6 hydrogen bonds, since the two d($G_4T_4G_4$) monomers of Oxy-1.5 are symmetry related. As in the analogous protein experiment (Cordier and Grzesiek, 1999; Cornilescu et al., 1999a), slight variations of the intraresidue $^{1}J_{N1C6}$ coupling constants lead to an incomplete suppression of five of the eight intranucleotide one-bond correlations. For comparison, the reference H(N)CO spectrum (Figure 2, pulse scheme B) is depicted in Figure 3B showing only correlations resulting from these intraresidue $^{1}J_{N1C6}$ couplings. The assignments for the eight $^{3h}J_{NC'}$ correlations agree

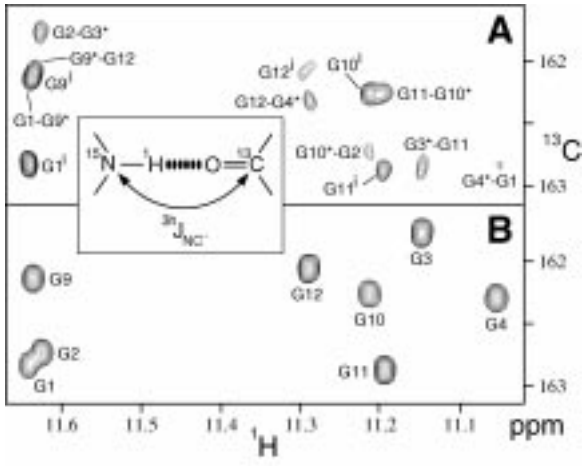

Figure 3. Quantitative-$J_{NC'}$ H(N)CO spectra of the uniformly ^{13}C/^{15}N-labeled DNA quadruplex. Resonances are labeled with assignment information. Due to the symmetry of Oxy-1.5, resonances are degenerate for two guanine bases Gi and Gi* located on different d($G_4T_4G_4$) oligonucleotides. (A) Resonances observed from recording a spectrum with pulse scheme A in Figure 2. Resonances in this panel result from magnetization transfer across the hydrogen bond between the donor imino ^{15}N1 and acceptor carbonyl ^{13}C6 nuclei for each G–G* base pair. Nucleotide names marked by the superscript i denote incomplete refocusing of the intranucleotide $^{1}J_{N1C6}$ coupling. The insert illustrates the definition of the scalar $^{3h}J_{N1C6}$ coupling via the hydrogen bond. (B) Reference spectrum recorded by using pulse scheme B of Figure 2. In this panel, resonances arise from the active covalent one-bond intranucleotide coupling between the imino ^{15}N1 and the carbonyl ^{13}C6 ($^{1}J_{N1C6}$). Contour lines in panel B are drawn at a 14.5 times higher level (corrected for different total experimental time) and the spacing between contour lines corresponds to a factor of 1.12 (A) and 1.2 (B).

with the base pairing scheme observed in the NMR structure (Smith and Feigon, 1992; Schultze et al., 1994) and the new crystal structure (M. Horvath and S. Schultz, personal communication).

The quantitative J-correlation pulse scheme in Figure 2 only determines the absolute value of $^{3h}J_{NC'}$, whereas the sign of the corresponding $^{3h}J_{NC'}$ coupling in proteins was determined as negative by a zero-quantum/double-quantum technique (Cornilescu et al., 1999b). Due to the inherent low sensitivity of the latter experiment, such a determination of the sign of $^{3h}J_{NC'}$ was not attempted for the Oxy-1.5 molecule. An accurate determination of the absolute value of $^{3h}J_{NC'}$ was only possible in six of the eight non-equivalent imino groups because of spectral overlap with the residual intranucleotide $^{1}J_{N1C6}$ correlations. Table 1 lists these individual $^{3h}J_{NC'}$ values, which range between 0.18 and 0.26 Hz with an estimated statistical error of approximately 0.02 Hz.

Table 1. $^{3h}J_{NC'}$ values for the Oxy-1.5 molecule at 298 K derived from the selective H(N)CO

Groove	Outer quartet	$^{3h}J_{NC'}$ (Hz)	Inner quartet	$^{3h}J_{NC'}$ (Hz)
Wide	G1-G9*[a]	nd[b]	G2-G3*	0.26±0.02
Medium	G9*-G12	nd	G3*-G11	0.21±0.02
Narrow	G12-G4*	0.20±0.02[c]	G11-G10*	0.24±0.03
Medium	G4*-G1	0.18±0.02	G10*-G2	0.21±0.02

[a]Gi-Gj* refers to donor base i and acceptor base j*. G and G* are located on different d($G_4T_4G_4$) oligonucleotides. Each Gi-Gj* pair has a symmetry related Gi*-Gj base pair.
[b]nd = not determined.
[c]Statistical errors as propagated from the noise in the individual experiments.

$^{2h}J_{NN}$ couplings

In addition to the imino to O6=C6 hydrogen bonds, the guanosine quartets contain hydrogen bonds between the amino ^{15}N2 donor and the ^{15}N7 acceptor atoms (Figure 1B). $^{2h}J_{NN}$ correlations across hydrogen bridges involving amino groups have recently been observed in an A-A base pair by means of a pseudo-heteronuclear H(N)N-COSY (Majumdar et al., 1999). As has been pointed out by Majumdar and co-workers (1999), limitations in the achievable ^{15}N RF power render a conventional homonuclear H(N)N-COSY experiment (Dingley and Grzesiek, 1998; Pervushin et al., 1998) inefficient for the detection of amino to aromatic $^{2h}J_{NN}$ couplings. They therefore designed a pseudo-heteronuclear H(N)N-COSY experiment where selective ^{15}N pulses excite the amino and aromatic ^{15}N resonances separately (Majumdar et al., 1999). An inconvenience of that experiment is that the resonances corresponding to the amino ^{15}N nuclei could not be detected and a separate spin-echo difference experiment was used to quantify the $^{2h}J_{NN}$ values.

The pulse scheme in Figure 4 is an improved version of the heteronuclear H(N)N-COSY which detects resonances of both amino and aromatic ^{15}N nuclei in a single experiment. Using as an example the evolution under the $^{2h}J_{NN}$ coupling between amino-^{15}N2 and aromatic ^{15}N7 nuclei in the G-G base pair, $2H2_zN2_x$ magnetization at point *a* is transferred to a term proportional to $4H2_zN2_yN7_z \sin(2\pi^{2h}J_{NN}T) + 2H2_zN2_x \cos(2\pi^{2h}J_{NN}T)$ at point *b* in Figure 4. Selective 180° ^{15}N pulses are applied separately at amino (82 ppm) and aromatic frequencies (232 ppm) in the middle of the transfer interval 2T. At the time point *b*, two selective $90^\circ_{\phi2}$ ^{15}N pulses are applied simultaneously at these frequencies such that the magnetization is transferred to $-4H2_zN2_zN7_y \sin(2\pi^{2h}J_{NN}T) + 2H2_zN2_x \cos(2\pi^{2h}J_{NN}T)$ at point *c*. After a normal frequency labelling period during t_1 and a second pair of simultaneous selective $90^\circ_{\phi3}$ ^{15}N pulses at point *d*, both terms are transferred back to observable $H2_y$ magnetization at point *e* which is proportional to $-\sin^2(2\pi^{2h}J_{NN}T)\cos(\omega_{N7}t_1) + \cos^2(2\pi^{2h}J_{NN}T)\cos(\omega_{N2}t_1)$. In order to achieve the proper phase-sensitive detection of ω_{N7} and ω_{N2} frequencies during the t_1-period, it is necessary to apply the ^{15}N $90^\circ_{\phi2}$ and $90^\circ_{\phi3}$ pulses in a phase coherent mode on both frequencies for every point of the t_1-evolution period. If this condition is fulfilled, the experiment yields results which are identical to the homonuclear H(N)N-COSY experiment (Dingley and Grzesiek, 1998) with diagonal peaks appearing in the two-dimensional spectrum at frequencies (ω_{N2},ω_{H2}) and cross peaks appearing at frequencies (ω_{N7},ω_{H2}). Note, however, that the ω_{N2} and ω_{N7} frequencies are measured relative to the two different carrier positions at 82 ppm and 232 ppm, respectively. As in the case of the homonuclear H(N)N-COSY, the value of $^{2h}J_{N2N7}$ is given by $\text{atan}((I_{N7}/I_{N2})^{1/2})/(2\pi T)$, where I_{N7}/I_{N2} is the ratio of the cross peak and diagonal peak intensities.

In principle, phase coherence on amino and aromatic frequencies can be achieved easily by using two separate ^{15}N radio frequency channels. If such a second ^{15}N channel is not available, phase coherence can also be achieved with no effort by the use of suitable phase-modulated $90^\circ_{\phi2}$ and $90^\circ_{\phi3}$ pulses and by setting the t_1-increment to a value of $n/\Delta f$, where Δf is the frequency difference of the carrier positions for the amino and aromatic resonances (150 ppm $*$ 60.8 MHz = 9120 Hz at 14.7 T) and n is an integer. For the experiment depicted in Figure 5, the ^{15}N-carrier was set to 82 ppm during the entire experiment and the $90^\circ_{\phi2}$ and $90^\circ_{\phi3}$ pulse pairs were generated from normal rectangular pulses by multiplication with a phase modulation factor in the form $[1 + \exp(i2\pi\Delta f\, t)]$. An RF field strength of $\Delta f/\sqrt{15}$ for these pulses achieves minimal cross excitation of amino and aromatic frequencies. Note that, due to the finite length of the pulses, an additional constant phase correction $\Delta\phi$ is necessary for one of the two frequencies, if an arbitrary initial t_1-delay is desired such as to ensure a suitable phase correction for the ω_1-frequency domain. For the specified rectangular pulses, an initial t_1-delay of $n/(2\Delta f)$ and $n = 8$, $\Delta\phi$ is calculated as -95.2°. This additional constant phase correction is easily incorporated into

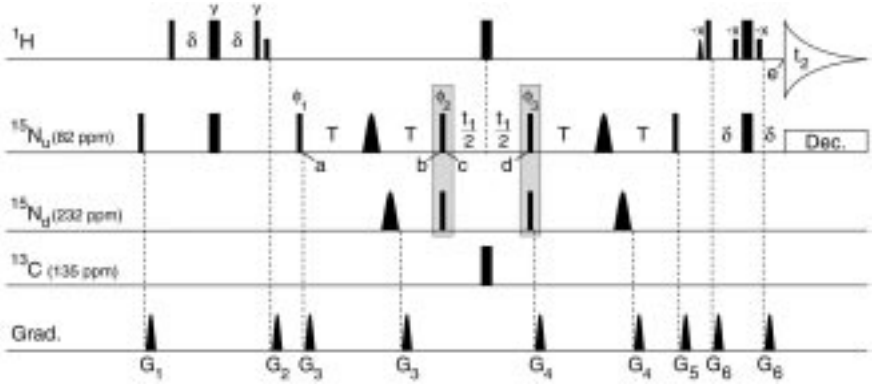

Figure 4. Pulse sequence for the quantitative-J_{NN} pseudo-homonuclear H(N)N-COSY experiment. Narrow and wide pulses correspond to flip angles of 90° and 180° respectively, and unless indicated, the phase is x. Carrier positions are ^1H_2O (^{1}H), 82 ppm (^{15}N), and 135 ppm (^{13}C). All regular ^{1}H, ^{15}N, and ^{13}C pulses are applied at an RF field strength of 29, 2.35, and 16.7 kHz, respectively. Rectangular low-power ^{1}H pulses are applied using $\gamma_H B_1/2\pi = 200$ Hz, and the sine-bell shaped $90°_{-x}$ pulse has a duration of 3.0 ms. ^{15}N 180° shaped pulses applied at the midpoint of the COSY transfer periods on both the upfield (N7) and downfield (N2) nitrogen nuclei have the shape of the center lobe of a (sin*x*)/*x* function with durations of 600 μs. The pair of ^{15}N pulses in each of the shaded boxes represents a rectangular pulse, phase-modulated such that it corresponds to two rectangular ^{15}N pulses with carrier positions at 82 and 232 ppm, respectively (see text). An RF field amplitude of 2.35 kHz is used for both pulses. WALTZ decoupling ($\gamma_N B_2/2\pi = 1.25$ kHz) was applied during acquisition on the ^{15}N channel. Delay durations: $\delta = 2.25$ ms; T = 20 ms. Phase cycling: ϕ_1 = y, −y; ϕ_2 = 2(x), 2(−x); ϕ_3 = 4(x), 4(−x); receiver = x, −x. Quadrature detection in the t_1 period was achieved by altering ϕ_1 and ϕ_2 in the States-TPPI manner. Gradients are sine-bell shaped, with an absolute amplitude of 25 G/cm at their center and durations (polarities) of $G_{1,2,3,4,5,6}$ = 2.8(+), 2.0(+), 0.3(−), 0.45(+), 2.0(−), and 0.4(+) ms.

one of the two shaped pulse pairs by setting the phase modulation factor to [1 + exp(i ($2\pi\Delta f\, t + \Delta\phi$))]. If these considerations are taken into account, in-phase detection of both ω_{N7} and ω_{N2} frequencies during t_1 is achieved by a normal States-TPPI incrementation (Marion et al., 1989) of phases ϕ_1 and ϕ_2.

Figure 5 shows the result of such a 4 h quantitative pseudo-homonuclear H(N)N-COSY experiment for the DNA quadruplex at 274 K. Clearly, cross peaks corresponding to N7 resonances and diagonal peaks corresponding to the amino N2 resonances are detected at the same time with reasonable sensitivity for four out of a total of eight non-equivalent amino groups. Note that the two sets of resonances correspond to two different ^{15}N frequency scales. Strong chemical exchange broadening resulting from rotations of the N2-amino groups causes the absence of diagonal and cross correlations for the G2, G4, and G12 amino-N2 groups. Due to this exchange, the diagonal peaks for the G9 amino group are also considerably weakened (Figure 5) and cross peaks to the ^{15}N7-nuclei of G12* are only detected in a 12 h experiment (not shown). Apparently this type of chemical exchange is centered at the two corners of the Oxy-1.5 molecule where the equivalent G4 and G4* residues are located. Table 2 lists individual $^{2h}J_{N2N7}$ values as determined from several H(N)N-COSY experiments at 274 K and 288 K. At these two temperatures, $^{2h}J_{N2N7}$ constants for the G-tetrads range between 6 and 8 Hz. An independent determination of the $^{2h}J_{N2N7}$ constants by the quantitative spin-echo technique (Majumdar et al., 1999) yields essentially identical values at 274 K (Table 2).

Discussion

Imino-carbonyl hydrogen bonding pattern in the G-quartets

Comparison of the cross peaks in the long-range H(N)CO (Figure 3A) and reference H(N)CO (Figure 3B) experiments reveals that a complete set of intra- and internucleotide N-H···O=C correlations can be traced around each of two quartets, i.e. G1(H1)→G9*(C6), G9*(C6)→G9*(H1), G9*(H1)→G12(C6), G12(C6)→G12(H1), G12(H1)→G4*(C6), G4*(C6)→G4*(H1), G4*(H1)→G1(C6), G1(C6)→G1(H1) for the outer quartet and similarly G2→G3*→G11→ G10*→G2 for the inner quartet. This establishes not only the G-quartet structure and the number of non-symmetry related G-quartets, but also the hydrogen bonding partners in the G-quartet. With the two non-symmetry related G-quartets connected via scalar couplings, assignments to specific bases are trivial since only one guanine has to be assigned to unambiguously get the rest. Once the hy-

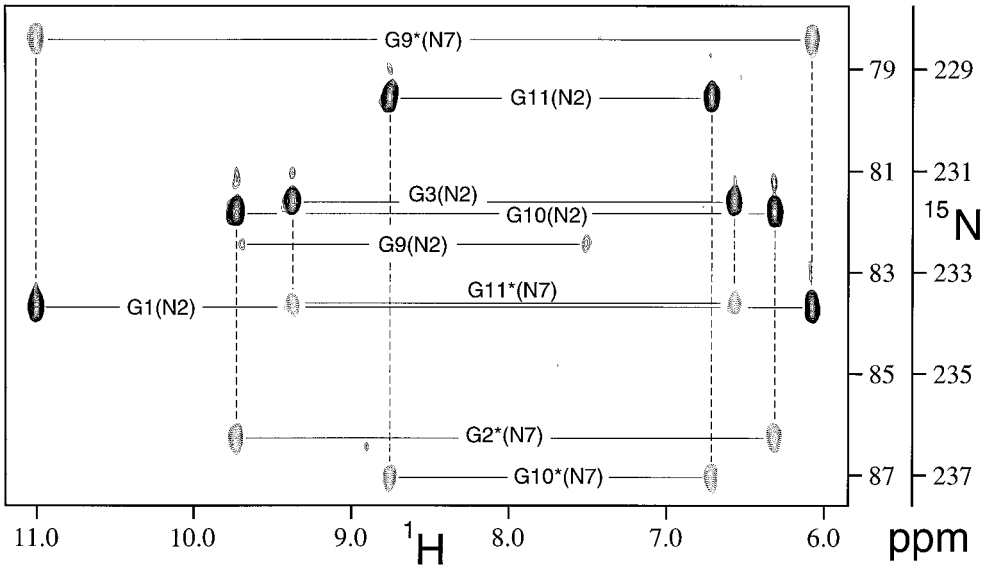

Figure 5. Quantitative-J_{NN} pseudo-homonuclear H(N)N-COSY spectrum of the uniformly $^{13}C/^{15}N$-labeled DNA quadruplex. Positive contours depict diagonal resonances, and negative contours (dashed lines) correspond to cross peaks resulting from $^{2h}J_{NN}$ couplings between the amino $^{15}N2$ (∼82 ppm) and aromatic $^{15}N7$ (∼232 ppm) nitrogens. Resonances are labeled with assignment information. For each amino group, pairs of resonances are observed corresponding to detection via the upfield or downfield amino $^{1}H2$ protons. Due to the peculiarity of the experiment, the inner ^{15}N frequency scale applies to the diagonal resonances whereas the outer frequency scale corresponds to the ^{15}N frequencies of the cross peaks.

drogen bonds are established via the J-coupling, correlation of the imino protons to the assigned base H8 protons can be obtained using a heteronuclear TOCSY (Sklenar et al., 1996). Note that the donor–acceptor pattern is clockwise around the outer quartets (G1-G9*-G12-G4*-G1) and counter-clockwise around the inner quartets (G2-G3*-G11-G10*-G2). Although the $^{3h}J_{NC'}$ are all rather small, the inner quartets show slightly larger couplings than the outer quartets (Table 1).

Comparison of $^{3h}J_{NC'}$ couplings in proteins and nucleic acids

An unexpected result of this study is that the $^{3h}J_{NC'}$ couplings of ∼0.2 Hz for the G-G base pairs are smaller on average than the equivalent $^{3h}J_{NC'}$ couplings observed in proteins. As the Oxy-1.5 molecule is an exceptionally stable DNA dimer with very little indication of local mobility on the pico- to nano- or millisecond time scale revealed by imino ^{15}N relaxation measurements (data not shown), motional averaging is an unlikely cause for the small values of $^{3h}J_{NC'}$. Apparently this difference in $^{3h}J_{NC'}$ for proteins and the Oxy-1.5 molecule is a consequence of differences in the overlap of donor, hydrogen, and acceptor orbitals which could be caused by both the different chemical environment of the donor and acceptor groups and by the different local geometry of the C=O···H–N hydrogen bonds.

An analysis of the new 1.9 Å X-ray structure of Oxy-1.5 (M. Horvath and S. Schultz, unpublished coordinates) shows that the average $R_{N1\cdots O6}$ and $R_{H1\cdots O6}$ (assuming $R_{N1H1} = 1.04$ Å and standard geometry) distances for the G–G base pairs are 2.91 ± 0.12 Å (N = 16) and 1.93 ± 0.12 Å (N = 16), respectively. Both these distances are very close to average N-O and H···O distances found in backbone hydrogen bonds of protein G (Cornilescu et al., 1999b), ubiquitin (Cordier and Grzesiek, 1999), and many other proteins (Baker and Hubbard, 1984) where absolute $^{3h}J_{NC'}$ values can be as large as 0.9 Hz. Similarly, the average of the O6···H1–N1 angle for Oxy-1.5 (157 ± 6°, N = 16) is very close to the average of the O···H–N angle determined from the 1.1 Å X-ray structure of protein G (158 ± 12°, N = 38) (Derrick and Wigley, 1994). In contrast, the H···O=C angle differs strongly between protein G and the G-quartets: whereas for protein G the average of this angle amounts to 147 ± 16° (N = 38), in the Oxy-1.5 structure, this value is only 125 ± 5° (N = 16). In the Oxy-1.5 structure, the O···H vector deviates on average by only 1 ± 8° (N = 16) from the plane defined by the aromatic ring

Table 2. $^{2h}J_{NN}$ values for the Oxy-1.5 molecule at different temperatures

		HNN-COSY[a] 274 K	Spin-echo[b] 274 K	HNN-COSY[c] 288 K
G1-G9*[d]	d[e]	8.1[f] ± 0.1	8.2 ± 0.1	7.9 ± 0.1
	u	8.0 ± 0.2	8.2 ± 0.1	7.8 ± 0.1
G9*-G12	d	7.1 ± 0.7	6.9 ± 0.5	nd[g]
	u	7.3 ± 0.5	5.8 ± 0.4	nd
G12-G4*		nd	nd	nd
G4*-G1		nd	nd	nd
G2-G3*		nd	nd	nd
G3*-G11	d	6.8 ± 0.3	6.4 ± 0.1	5.9 ± 0.8
	u	6.6 ± 0.1	6.3 ± 0.1	6.1 ± 0.7
G11-G10*	d	6.6 ± 0.1	6.7 ± 0.1	6.3 ± 0.2
	u	6.3 ± 0.1	6.8 ± 0.1	6.2 ± 0.2
G10*-G2	d	6.9 ± 0.1	6.9 ± 0.1	6.6 ± 0.2
	u	6.9 ± 0.1	7.2 ± 0.1	6.8 ± 0.2

[a]Data are determined as the mean of three independent H(N)N-COSY experiments with experimental times of 4, 12, and 14 h, respectively. Errors are given as the variance of these three determinations. Values for the G9-G12* correlation could only be determined from the 12 and 14 h experiments.
[b]Data are determined from a 12 h quantitative spin-echo experiment (Majumdar et al., 1999). Statistical errors are estimated from the experimental noise.
[c]Data are determined from a 6 h H(N)N-COSY experiment. Statistical errors are estimated from the experimental noise.
[d]Gi-Gj* refers to donor base i and acceptor base j* located on different d($G_4T_4G_4$) monomer subunits. Corresponding Gi*-Gj base pairs are symmetry related.
[e]Chemical shift of the amino ^{1}H2 resonance from which the $^{2h}J_{NN}$ coupling was determined: downfield (d), upfield (u).
[f]Absolute values in Hz.
[g]nd = not determined due to exchange broadening.

of the acceptor group whereas for protein G this deviation of the O···H vector from the acceptor peptide plane amounts to 14 ± 26° (N = 38). Therefore, in the G-quartet the O···H vector points almost exactly into the direction of the idealized sp^2 oxygen lone pair orbital (120° in-plane H···O=C angle) whereas in protein G and other proteins (Baker and Hubbard, 1984) the O···H vector deviates substantially from this ideal sp^2 orbital direction and points more into the direction of the C=O vector.

Although a recent quantum-chemical study (Scheurer and Brüschweiler, 1999) shed light on the dependence of the $^{3h}J_{NC'}$ coupling on the O···H–N angle, with the strongest couplings being expected for a linear geometry, the dependence of $^{3h}J_{NC'}$ on the H···O=C angle has not been described and remains poorly understood. The observation of the smaller absolute values for $^{3h}J_{NC'}$ in the G-quartets could be due to the difference in the H···O=C angle where the deviation from linearity would lead to reduced orbital overlap between the lone pair participating in the hydrogen bond and the carbon sp^2-hybrid participating in the C=O double bond. Another possible explanation are genuine differences in the carbonyl and nitrogen electronic orbitals of the guanine and peptide moieties. Differences in the extent of the oxygen lone pair orbitals for the guanosine tetrad could result from the coordination of Na^+ ions that are bound in the center of the quadruplex. A recent 0.9 Å resolution crystal structure of a parallel four stranded quadruplex (Phillips et al., 1997) indicates that the Na^+ ions are located either in the plane of the quartets or between two quartets and coordinate to the electron lone pair of the carbonyl oxygen, which is not participating in the H1···O6=C6 hydrogen bond. Presumably this cation coordination could withdraw electron density from the hydrogen bond and lead to reduced overlap between the oxygen and the hydrogen orbitals.

$^{2h}J_{NN}$ *couplings*

The $^{2h}J_{N2N7}$ values for the DNA-quadruplex are very similar in size to $^{2h}J_{NN}$ values of 6–8 Hz observed for hydrogen-bonded imino ^{15}N nuclei in Watson–Crick and Hoogsteen base pairs (Dingley and Grzesiek, 1998; Pervushin et al., 1998; Dingley et al., 1999) Correspondingly, the average $R_{N2\cdots N7}$ distance of 2.88 ± 0.14 Å (N = 16) as calculated from the 1.9 Å resolution X-ray crystal structure of Oxy-1.5 (M. Horvath and S. Schultz, unpublished coordinates) is very close to average donor–acceptor distances $R_{N1\cdots N3}$ of 2.92 Å and 2.81 Å observed for Watson–Crick G–C and T–A base pairs (Dingley et al., 1999). Interestingly, the size of the G1-G9* $^{2h}J_{N2N7}$ coupling is significantly larger (8.1 Hz) than the other $^{2h}J_{NN}$ couplings observed. In the new crystal structure of Oxy-1.5, this larger $^{2h}J_{N2N7}$ value coincides with a significantly shorter $R_{N2\cdots N7}$ distance of 2.65 Å for the G1-G9* base pair. Therefore, this experimental finding shows again that the size of the trans-hydrogen bond couplings can be correlated directly with donor–acceptor distances (Dingley and Grzesiek, 1998; Cordier and Grzesiek, 1999; Cornilescu et al., 1999b; Dingley et al., 1999; Scheurer and Brüschweiler, 1999). Apparently the shorter $R_{N2\cdots N7}$ distance for G1-G9* is not correlated with a stronger protection against exchange of the amino protons of G1 with water, because the slowest exchange is observed for the amino protons of G3 and G11 which

are part of the inner quartets (Smith and Feigon, 1993). This finding is remarkable but could be expected since solvent exchange rates of labile protons are strongly influenced by a number of factors such as solvent accessibility, the pK, and base pair opening rates (Teitelbaum and Englander, 1975; Kettani et al., 1997).

In B-DNA, the hydrogen-bonded and non-hydrogen-bonded guanine amino proton pairs are generally observed as one broad resonance due to intermediate-fast rotation around the C-N bond, as well as exchange with water. The observation of resolved resonances for the amino groups of G1, G3, G10 and G11 (Figure 5) in the quadruplex is therefore rather unusual. On the other hand, the amino group of G9 is affected to a large extent by exchange broadening from the C-N bond rotation at 274 K (Figure 5). Thus, it is striking that the $^{2h}J_{N2N7}$ constant for the G9-G12* correlation is not strongly reduced (∼6–7 Hz, Table 2). Similarly, almost no reduction in the value of $^{2h}J_{N2N7}$ (∼6 Hz) is observed for the G3-G11* base pair at 288 K where the G3-N2 amino group resonances are analogously broadened and weakened due to the onset of chemical exchange at this temperature (not shown). An explanation for this phenomenom could be that even in the presence of fast amino group rotations in the millisecond range, completely open states of the N2···N7 hydrogen bond are not highly populated. Since the H(N)N-COSY experiment only measures the ensemble average of electron-mediated magnetization transfer across the hydrogen bond, rotations on the millisecond time scale would not affect the value of $^{2h}J_{N2N7}$ provided that the average population of an open hydrogen bond is small in comparison to the two possible closed states.

The $^{2h}J_{N2N7}$ values found in the G-tetrad are significantly larger than the analogous amino ^{15}N6 to aromatic ^{15}N7 $^{2h}J_{NN}$ couplings of approximately 2.5 Hz reported for A–A mismatch base pairs in a DNA arrowhead motif for which a high resolution X-ray crystal structure is currently not available (Majumdar et al., 1999). This difference must be based either on the different chemical nature of the donor and acceptor groups or on a different hydrogen bond geometry in the A–A mismatch base pairs. Examples of N-H···N hydrogen bonds in many different base pair types show that the $^{2h}J_{NN}$ is rather insensitive with respect to the position of the donor and acceptor nitrogen atoms in the aromatic ring system of nucleic acids. For donor–acceptor distances of ∼2.8–2.9 Å, values for $^{2h}J_{NN}$ of 6–8 Hz have been observed for the imino hydrogen bonds of Watson–Crick G-C, U-A, and T-A (Dingley and Grzesiek, 1998; Pervushin et al., 1998), reverse Hoogsteen U-A (Wöhnert et al., 1999), Hoogsteen T-A (Dingley et al., 1999) base pairs and also for the amino hydrogen bonds in the G-quartet. Therefore, it seems more likely that the much smaller $^{2h}J_{NN}$ couplings for A–A mismatch base pairs are caused by a different geometry of the hydrogen bond which leads to reduced overlap between donor, hydrogen and acceptor electronic orbitals.

Acknowledgements

We thank Martin Horvath and Steve Schultz for access to the coordinates for the crystal structure of Oxy-1.5 prior to publication and Florence Cordier and Karsten Theis for valuable discussions. A.J.D. is a recipient of an Australian National Health and Medical Research Council C.J. Martin Fellowship (Regkey 987074). This work was funded by DFG grant GR1683/1–1 to S.G. and NIH grants GM37254 and GM48123 to J.F.

References

Abragam, A. (1961) *The Principles of Nuclear Magnetism*, Clarendon Press, Oxford.
Allain, F.H.-T. and Varani, G. (1995) *J. Mol. Biol.*, **250**, 333–353.
Baker, E.N. and Hubbard, R.E. (1984) *Prog. Biophys. Mol. Biol.*, **44**, 97–179.
Blake, P.R., Lee, B., Summers, M.F., Adams, M.W., Park, J.B., Zhou, Z.H. and Bax, A. (1992a) *J. Biomol. NMR*, **2**, 527–533.
Blake, P.R., Park, J.-B., Adams, M.W. and Summers, M.F. (1992b) *J. Am. Chem. Soc.*, **114**, 4931–4933.
Brünger, A. (1992) XPLOR, Yale University, New Haven, CT, U.S.A.
Butcher, S.E., Allain, F.H.-T. and Feigon, J. (1999) *Nat. Struct. Biol.*, **6**, 212–216.
Cate, J.H., Gooding, A.R., Podell, E., Zhou, K., Golden, B.L., Kundrot, C.E., Cech, T.R. and Doudna, J.A. (1996) *Science*, **273**, 1678–1685.
Cordier, F. and Grzesiek, S. (1999) *J. Am. Chem. Soc.*, **121**, 1601–1602.
Cordier, F., Rogowski, M., Grzesiek, S. and Bax, A. (1999) *J. Magn. Reson.*, **140**, 510–512.
Cornilescu, G., Hu, J.-S. and Bax, A. (1999a) *J. Am. Chem. Soc.*, **121**, 2949–2950.
Cornilescu, G., Ramirez, B.E., Frank, M.K., Clore, G.M., Gronenborn, A.M. and Bax, A. (1999b) *J. Am. Chem. Soc.*, **121**, 6275–6279.
Crabtree, R., Siegbahn, P., Eisenstein, O., Rheingold, A. and Koetzle, T. (1996) *Acc. Chem. Res.*, **29**, 348–354.
Delaglio, F., Grzesiek, S., Vuister, G.W., Zhu, G., Pfeifer, J. and Bax, A. (1995) *J. Biomol. NMR*, **6**, 277–293.
Derrick, J.P. and Wigley, D.B. (1994) *J. Mol. Biol.*, **243**, 906–918.
Dieckmann, T. and Feigon, J. (1997) *J. Biomol. NMR*, **9**, 259–272.

Dingley, A. and Grzesiek, S. (1998) *J. Am. Chem. Soc.*, **120**, 8293–8297.
Dingley, A.J., Masse, J.E., Peterson, R.D., Barfield, M., Feigon, J. and Grzesiek, S. (1999) *J. Am. Chem. Soc.*, **121**, 6019–6027.
Emsley, L. and Bodenhausen, G. (1990) *Chem. Phys. Lett.*, **165**, 469–476.
Fang, G. and Cech, T.R. (1993a) *Cell*, **74**, 875–885.
Fang, G. and Cech, T.R. (1993b) *Biochemistry*, **32**, 11646–11657.
Garrett, D.S., Powers, R., Gronenborn, A.M. and Clore, G.M. (1991) *J. Magn. Reson.*, **95**, 214–220.
Gesteland, R.E. and Atkins, J.F. (1993) *The RNA World*, Cold Spring Harbor Laboratory Press, Plainview, NY.
Giraldo, R. and Rhodes, D. (1994) *EMBO J.*, **13**, 2411–2420.
Golubev, N.S., Shenderovich, I.G., Smirnov, S.N., Denisov, G.S. and Limbach, H.-H. (1999) *Chem. Eur. J.*, **5**, 492–497.
Guschlbauer, W., Chantot, J.-F. and Thiele, D. (1990) *J. Biomol. Struct. Dyn.*, **8**, 491–511.
Ippel, J.H., Wijmenga, S.S., de Jong, R., Heus, H.A., Hilbers, C.W., de Vroom, E., van der Marel, G.A. and van Boom, J.H. (1996) *Magn. Reson. Chem.*, **34**, S156–S176.
Isaacs, E.D., Shukla, A., Platzman, P.M., Hamann, D.R., Barbiellini, B. and Tulk, C.A. (1999) *Phys. Rev. Lett.*, **82**, 600–603.
Kang, C., Zhang, X., Ratliff, R., Moyzis, R. and Rich, A. (1992) *Nature*, **356**, 126–131.
Kettani, A., Gueron, M. and Leroy, J.-L. (1997) *J. Am. Chem. Soc.*, **119**, 1108–1115.
Kwon, O. and Danishefsky, S. (1998) *J. Am. Chem. Soc.*, **120**, 1588–1599.
Majumdar, A., Kettani, A. and Skripkin, E. (1999) *J. Biomol. NMR*, **14**, 67–70.
Marion, D., Ikura, M., Tschudin, R. and Bax, A. (1989) *J. Magn. Reson.*, **85**, 393–399.
Masse, J., Bortmann, P., Dieckmann, T. and Feigon, J. (1998) *Nucleic Acids Res.*, **26**, 2618–2624.
Pauling, L. (1949) *J. Chim. Phys.*, **46**, 435.
Pervushin, K., Ono, A., Fernandez, C., Szyperski, T., Kainosho, M. and Wüthrich, K. (1998) *Proc. Natl. Acad. Sci. USA*, **95**, 14147–14151.
Pervushin, K., Riek, R., Wider, G. and Wüthrich, K. (1997) *Proc. Natl. Acad. Sci. USA*, **94**, 12366–12371.
Phillips, K., Dauter, Z., Murchie, A.I., Lilley, D.M. and Luisi, B. (1997) *J. Mol. Biol.*, **273**, 171–182.
Saenger, W. (1984) *Principles of Nucleic Acid Structure*, Springer-Verlag, New York, NY.
Scheurer, C. and Brüschweiler, R. (1999) *J. Am. Chem. Soc.*, **121**, 8661–8662.
Schultze, P., Smith, F.W. and Feigon, J. (1994) *Structure*, **2**, 221–233.
Shenderovich, I.G., Smirnov, S.N., Denisov, G.S., Gindin, V.A., Golubev, N.S., Dunger, A., Reibke, R., Kirpekar, S., Malkina, O.L. and Limbach, H.-H. (1998) *Ber. Bunsenges. Phys. Chem.*, **102**, 422–428.
Sklenar, V., Dieckmann, T., Butcher, S.E. and Feigon, J. (1996) *J. Biomol. NMR*, **7**, 83–87.
Smirnov, S., Benedict, H., Golubev, N., Denisov, G., Kreevoy, M., Schowen, R. and Limbach, H.-H. (1999) *Can. J. Chem.*, **77**, 943–949.
Smith, F.W. and Feigon, J. (1992) *Nature*, **356**, 164–168.
Smith, F.W. and Feigon, J. (1993) *Biochemistry*, **32**, 8682–8692.
Teitelbaum, H. and Englander, S.W. (1975) *J. Mol. Biol.*, **92**, 79–92.
Varani, G., Aboul-ela, F. and Allain, F.H.-T. (1996) *Prog. NMR Spectrosc.*, **29**, 51–127.
Wang, Y.X., Jacob, J., Cordier, F., Wingfield, P., Stahl, S.J., Lee-Huang, S., Torchia, D., Grzesiek, S. and Bax, A. (1999) *J. Biomol. NMR*, **14**, 181–184.
Wöhnert, J., Dingley, A.J., Stoldt, M., Görlach, M., Grzesiek, S. and Brown, L.R. (1999) *Nucleic Acids Res.*, **27**, 3104–3110.
Zahler, A.M., Williamson, J.R., Cech, T.R. and Prescott, D.M. (1991) *Nature*, **350**, 718–720.